Many-Electron System on Helium and Color Center Spectroscopy

A. D. Chepelianskii,[1] D. Konstantinov,[2] and M. I. Dykman[3]
[1]LPS, Université Paris-Saclay, CNRS, UMR 8502, F-91405 Orsay, France
[2]Okinawa Institute of Science and Technology (OIST) Graduate University, Onna, Okinawa 904-0412, Japan
[3]Department of Physics and Astronomy, Michigan State University, East Lansing, Michigan 48824, USA

(Received 11 November 2020; revised 16 April 2021; accepted 18 May 2021; published 28 June 2021)

Electrons on the helium surface display sharp resonant absorption lines related to the transitions between the subbands of quantized motion transverse to the surface. A magnetic field parallel to the surface strongly affects the absorption spectrum. We show that the effect results from admixing the intersubband transitions to the in-plane quantum dynamics of the strongly correlated electron liquid or a Wigner crystal. This is similar to the admixing of electron transitions in color centers to phonons. The spectrum permits a direct characterization of the many-electron dynamics and also enables testing the theory of color centers in a system with controllable coupling.

DOI: 10.1103/PhysRevLett.127.016801

Electrons above the surface of liquid helium are localized in a one-dimensional potential well, which is formed by the high repulsive barrier at the surface and the image potential. The energy levels in the well are quantized. The electrons occupy the lowest level forming a two-dimensional system [1,2]. The spectroscopic observation of transitions between the quantized energy levels [3] was a direct proof of the picture of the electron confinement and the overall nature of the potential. Since then much work has been done on the exact positions and the widths of the spectral lines and their dependence on the temperature and the electron density [4–12].

The electron system on helium is free from static disorder. It is also weakly coupled to the vibrational excitations in helium, ripplons and phonons. The observed spectral lines are narrow, with width as small as $\sim$2 MHz for $T = 0.3$ K [8]. In the nomenclature of the solid-state spectroscopy they correspond to zero-phonon lines. Such lines in the spectra of point defects result from transitions between the defect energy levels with no energy transfer to or from phonons [13]. The physics of point defects and the defect spectroscopy have been the focus of attention recently in the context of quantum computing and quantum sensing [14]. On their side, electrons on helium themselves have been also considered as a viable candidate system for a scalable quantum computer [15–19].

One of the major attractive features of electrons on helium is the possibility to study many-electron effects. The electron-electron interaction is strong, the ratio of its energy to the electron kinetic energy is $\Gamma = e^2(\pi n_s)^{1/2}/k_B T > 30$ for the electron density $n_s \geq 10^7$ cm^{-2} and $T \leq 0.3$ K. The electrons form a Wigner crystal [20,21] or a classical or quantum nondegenerate liquid with unusual transport properties, cf. Refs. [22–29] and references therein. Spectroscopy would be expected to provide a most detailed insight into the correlated many-electron dynamics. However, the only spectral effect of the electron-electron interaction studied so far is a small density-dependent line shift [5,10].

In this Letter we show that, by applying a magnetic field along the helium surface, one can use spectroscopy to study quantum dynamics of a nondegenerate electron liquid and a Wigner solid. Importantly, in the cases where this dynamics has been already understood, the system can serve as a quantum simulator of color center spectroscopy, with the unique opportunity of controlling the strength of the coupling of the electron transition and many-body excitations in the system. The importance of such simulations follows from the broad applications of color centers, including the color centers in diamond such as NV centers, cf. Refs. [14,30,31].

The change of the interband absorption spectrum by an in-plane magnetic field has been studied for degenerate quasi-two-dimensional electron systems in semiconductors, see Ref. [32] and references therein. The results were interpreted in the mean-field approximation. The field-induced high-temperature spectral broadening was also reported for electrons on helium [33,34]. Here we show that, for electrons on helium in the quantum regime, the spectrum is qualitatively different from what the mean-field theory predicts. It has to be analyzed using an approach that explicitly takes into account the interplay of the strong correlations and fluctuations in the quantum electron system.

The effect of the parallel magnetic field on the electron spectrum and the similarity with the physics of color centers can be understood from Fig. 1. We choose the z axis as the direction of quantized motion normal to the surface. In different quantized states of the out-of-plane motion $|\mu\rangle$ the electron is at a different average distance

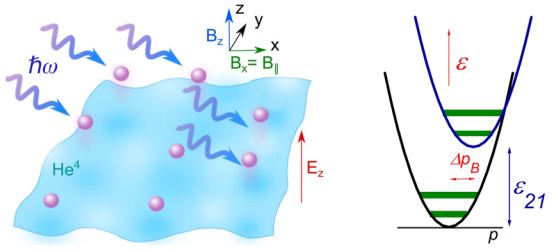

FIG. 1. Left: The many-electron system on helium in a magnetic field with components parallel ($B_\parallel \equiv B_x$) and perpendicular ($B_\perp \equiv B_z$) to the helium surface. Right: The energy spectrum of an electron in the two lowest bands of motion normal to the surface. The energy difference between the bands ε_{21} is the distance between the levels of the quantized motion along the z axis. The single-electron kinetic energy of motion along the surface is quadratic in the in-plane momentum $\mathbf{p}$ for $B_\perp = 0$. The field $B_\perp$ transforms the spectrum into the Landau levels, which are broadened by the electron-electron interaction. The field $B_\parallel$ shifts the bands of the in-plane motion by Δp_B, see Eq. (1).

from the surface. If a magnetic field $B_\parallel$ is applied parallel to the surface, an interstate transition leads to the electron shift transverse to $B_\parallel$. Therefore the electron in-plane momentum is changed by the Lorentz force in the $\hat{\mathbf{z}} \times \mathbf{B}_\parallel$ direction. For the transition $|1\rangle \to |2\rangle$ from the ground to the first excited state the change Δp_B is

$$\Delta p_B = m\omega_\parallel \Delta_z, \qquad \Delta_z = \bar{z}_{22} - \bar{z}_{11},$$
$$\omega_\parallel = eB_\parallel/mc, \qquad \bar{z}_{\mu\mu} = \langle \mu|z|\mu\rangle \quad (\mu = 1, 2). \tag{1}$$

Thus the minima of the energy bands $\varepsilon_1(\mathbf{p})$ and $\varepsilon_2(\mathbf{p})$ of the in-plane motion ($\mathbf{p}$ is the in-plane momentum) are shifted with respect to each other. We assume $m\omega_\parallel^2 \Delta_z^2 \ll \varepsilon_{21} \equiv \min[\varepsilon_2(\mathbf{p}) - \varepsilon_1(\mathbf{p})]$.

The right panel of Fig. 1 has the familiar form of the sketch of the energy of a point defect coupled to a vibrational mode in a crystal [13]. In the case of a defect, the horizontal axis is the coordinate of the vibrational mode, and the parabolas show the potential energy of the mode in the two electron states with the energy difference ε_{21}. The zero-phonon spectral line corresponds to a transition at frequency $\varepsilon_{21}/\hbar$ between the minima of the parabolas. The vertical transition from the minimum of the lower parabola (the Franck-Condon transition) occurs at a higher energy. Usually the electron is coupled to many modes (phonons), which significantly complicates the analysis, as has been known since the work of Pekar [35] and Huang and Rhys [36].

In distinction from a defect, the parabolas in Fig. 1 show the single-electron energy as a function of the in-plane momentum. In a strongly correlated electron system the momentum can be transferred to other electrons. Such recoil reminds us of the recoil from the absorption of a gamma-quantum by an impurity in a crystal, which underlies the Mössbauer effect. By analogy with the Mössbauer effect and the spectra of color centers, the absorption spectrum of electrons on helium should strongly depend on the in-plane many-electron dynamics.

To analyze the spectrum in the presence of strong electron correlations, one should start with the full Hamiltonian of the system. It is a sum of the terms $H_\parallel$, $H_\perp$, and H_i that describe, respectively, the in-plane motion, the motion normal to the helium surface in the image potential [1,2], and the coupling of these two motions by the in-plane field $B_\parallel \equiv B_x$. In the presence of a magnetic field $B_\perp \equiv B_z$ normal to the surface

$$H = H_\parallel + H_\perp + H_i,$$
$$H_\parallel = \sum_n \frac{\boldsymbol{\pi}_n^2}{2m} + \frac{1}{2}\sum_{n,m}{}' \frac{e^2}{|\mathbf{r}_n - \mathbf{r}_m|},$$
$$H_\perp = \sum_n \left[\frac{p_{nz}^2}{2m} + U(z_n)\right], \qquad H_i = \sum_n \omega_\parallel \pi_{ny}(z_n - \bar{z}_{11}).$$

Here n enumerates electrons, $\mathbf{r}_n \equiv (x_n, y_n)$ and $\boldsymbol{\pi}_n = -i\hbar\boldsymbol{\nabla}_n + (e/c)\mathbf{A}_\perp(\mathbf{r}_n)$ are the in-plane electron coordinate and kinematic momentum [$\mathbf{A}_\perp(\mathbf{r})$ is the vector-potential of the field $B_\perp \equiv B_z$], whereas $U(z)$ is the confining potential. The leading-order part of H_i is diagonal with respect to the states $|\mu\rangle_n$ of the out-of-plane motion, $H_i = \omega_\parallel \Delta_z \sum_n \pi_{ny} |2\rangle_{n\,n}\langle 2|$, see Supplemental Material [37].

The frequency $\varepsilon_{21}/\hbar$ of the interstate transition largely exceeds all characteristic frequencies of the in-plane electron motion. One therefore can think of the adiabatic approximation in which the transition $|1\rangle \to |2\rangle$ occurs "instantaneously" for a given in-plane many-electron state. The transition frequency depends on this state. It is this dependence that determines the shape of the spectrum.

Formally, the absorption of microwaves polarized in the z direction is determined by the real part of the conductivity $\sigma_{zz}(\omega)$. For a nondegenerate electron system it is given by the sum of the contributions from individual electrons, i.e., by the conductivity of an nth electron multiplied by the in-plane electron density n_s. From the Kubo formula

$$\mathrm{Re}\sigma_{zz}(\omega) = C_\sigma \mathrm{Re}\int_0^\infty dt e^{i\omega t}\langle [z_n(t), z_n(0)]\rangle. \tag{2}$$

Here, $C_\sigma = e^2 n_s \omega/\hbar \approx e^2 n_s \varepsilon_{21}/\hbar^2$ in the considered range of resonant absorption.

The evaluation of the conductivity depends on whether the electron system is a liquid or a crystal. For a Wigner crystal the operators $\boldsymbol{\pi}_n$ are linear combinations of the creation and annihilation operators of the Wigner crystal phonons, making the form of the coupling H_i and the problem as a whole largely the same as that of the spectra of color centers [37]. However, in our experiment the electron system is a strongly correlated liquid in a strong transverse

magnetic field $B_\perp$. In such a field the in-plane electron motion is a superposition of a fast quantized cyclotron motion at frequencies $\sim\omega_c = eB_\perp/mc$ and a slow semiclassical drift of the guiding centers of the cyclotron orbits. The drift comes from the fluctuational electric field caused by the electron density fluctuations. The field on an nth electron is $\mathbf{E}_n = -e\sum'_m(\mathbf{r}_n - \mathbf{r}_m)/|\mathbf{r}_n - \mathbf{r}_m|^3$. It varies on the timescale $\omega_c/\omega_p^2 \gg \omega_c^{-1}$, where $\omega_p = (2\pi e^2 n_s^{3/2}/m)^{1/2}$ [22].

The timescale separation allows describing the peak of the absorption spectrum of the electron liquid in an explicit form [37]. It is convenient to single out in the integrand in Eq. (2) the factor that oscillates at the resonant frequency, $\langle[z_n(t), z_n(0)]\rangle = |\langle 1|z|2\rangle|^2 \exp(-i\varepsilon_{21}t/\hbar)Q(t)$. The function $Q(t)$ describes the effect of the in-plane many-electron dynamics,

$$Q(t) = e^{i\delta_\parallel t}\exp[-(\gamma^2/2)w(t)],$$
$$\delta_\parallel = m\omega_\parallel^2\Delta_z^2/2\hbar, \qquad \gamma^2 = \delta_\parallel\omega_p^2 k_B T/2\pi\hbar\omega_c^2,$$
$$w(t) = (n_s^{3/2}k_B T)^{-1}\iint_0^t dt_1 dt_2\langle\mathbf{E}_n(t_1)\mathbf{E}_n(t_2)\rangle. \tag{3}$$

We assumed Gaussian distribution of the fluctuational field $\mathbf{E}_n$. In a broad parameter range relevant for the experiments on electrons on helium $\langle\mathbf{E}_n^2\rangle \approx F(\Gamma)n_s^{3/2}k_B T$, where $F(\Gamma) \simeq 9$.

If the coupling to the in-plane fluctuations is strong, $\gamma \gg \omega_p^2/\omega_c$, from Eq. (3) the main part of the absorption spectrum (2) is a Gaussian peak, reminiscent of the spectrum of color center. The typical width of the peak in the frequency units is $\gamma F(\Gamma)^{1/2}$.

The absorption spectrum also has an analog of the zero-phonon line. It is described by the long-time behavior of $w(t)$ and dominates the spectrum for small $B_\parallel$. In the electron liquid the line is Lorentzian with a half-width which, unexpectedly, is determined by the self-diffusion and is equal to $m\delta_\parallel D/2$, where D is the self-diffusion coefficient [37]. One can switch from a Lorentzian to a Gaussian spectrum by increasing the field $B_\parallel$.

In the experiment, the absorption spectrum is measured by varying the electric field E_z applied perpendicular to the helium surface, using that the level spacing ε_{21} linearly depends on E_z within the linewidth. In the units of E_z, the typical width of the Gaussian peak is

$$\delta E_z = \frac{B_\parallel}{B_\perp\sqrt{2}}[k_B T n_s^{3/2}F(\Gamma)]^{1/2}. \tag{4}$$

All parameters in Eq. (4) can be controlled in the experiment. This enables testing the theoretical prediction with high accuracy.

We measured the change of the low-frequency helium cell admittance Y due to absorption of microwave radiation, as explained in the Supplemental Material [37]. Such photoassisted transport spectroscopy provides a sensitive way to measuring resonant microwave absorption [10]. The method has been used to study the rich out-of-equilibrium physics and a variety of nontrivial nonlinear effects associated with moderately strong resonant microwave excitation of the electron system [10,12,27,28]. Here we focus on the linear response. The microwave power was attenuated down to μW levels. The experimental technique used here is very close to [12], however, improvements were made to work at very low microwave power and to ensure that the helium filling level in the sample cell was close to 50% to provide a good compensation between the electric field created by the top and bottom image charges. These steps are described in detail in the Supplemental Material [37].

The spectra of the resonant $|1\rangle \to |2\rangle$ photoexcitation are shown in Fig. 2. For $B_\parallel \gtrsim 0.4$ T, where the strong-coupling condition holds, the observed shape of the spectra is very well described by a Gaussian fit (dashed lines) with the variance δE_z given by Eq. (4), with no fitting parameters. The overall area of the spectral peaks is determined by the photoassisted transport response of electrons on helium, which depends on $B_\parallel$; the discussion of this dependence is beyond the scope of this Letter.

In Fig. 3 we show the linewidth δE_z as a function of $B_\parallel$ for several refrigerator temperatures. The observed linear dependence quantitatively agrees with Eq. (4) in the strong-coupling regime, which corresponds to $B_\parallel T^{1/2} \gtrsim 0.15$ T $\times$ K$^{1/2}$, for the used n_s and $B_\perp$. The linewidth at $B_\parallel = 0$ is attributed to residual inhomogeneous broadening in our system. The linear fits to the data at different temperatures all intersect near $B_\parallel = 0$, supporting this interpretation. The inset shows the ratio $\delta E_z/B_\parallel$ as a function of the square root of the temperature. The black line depicts this ratio as given by Eq. (4)

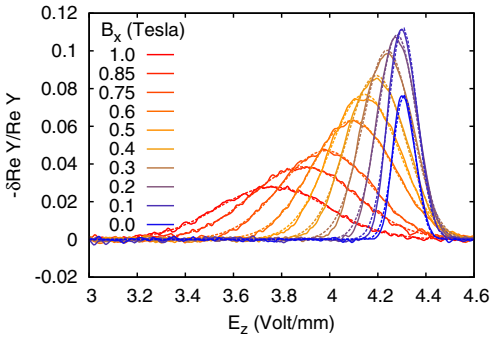

FIG. 2. The spectra of the relative microwave-induced change of the low-frequency admittance Y for different $B_\parallel \equiv B_x$. The data refer to the microwave frequency $f = 150$ GHz, $T = 0.2$ K, $B_\perp \equiv B_z = 0.5$ T, and $n_s = 21.5 \times 10^6$ cm^{-2}. The ac bias is 30 mV. The dashed lines show Gaussian fit to the data with the variance δE_z^2 given by Eq. (4).

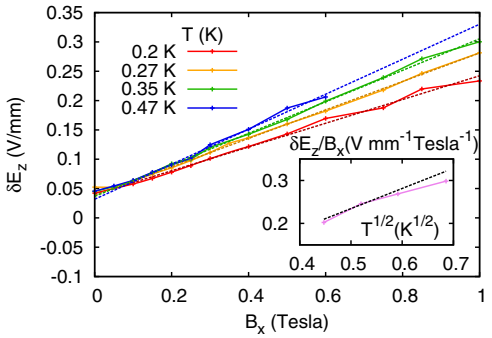

FIG. 3. The dependence of the typical width of the spectral peaks δE_z on $B_\parallel \equiv B_x$ for different temperatures. The other parameters are the same as in Fig. 2. The dashed lines are the linear fit. In the strong-coupling range they are described by Eq. (4). The inset shows the slope of $\delta E_z/B_\parallel$ as a function of $T^{1/2}$. The dashed black line is given by Eq. (4) with no adjustable parameters.

with no adjustable parameters [Eq. (4) holds for $T^{1/2} < (\hbar\omega_c/k_B)^{1/2} \approx 0.6\ \mathrm{K}^{1/2}$].

To further check Eq. (4) we investigated the density dependence of the linewidth for different magnetic fields $B_\parallel \equiv B_x$ and $B_\perp \equiv B_z$. In order to reduce the averaging time and increase the sensitivity for small n_s we used a stronger microwave power, in the 100 μW range. This resulted in an additional spectral broadening, which we attribute to an effective electron temperature $T_e = 0.6$ K (the refrigerator temperature is 0.3 K; the dependence of the linewidth on the microwave power is shown in the inset in Fig. 4). With this assumption the data are in full agreement with Eq. (4). As shown in Fig. 4, $(\delta E_z)^2 \propto n_s^{3/2}$.

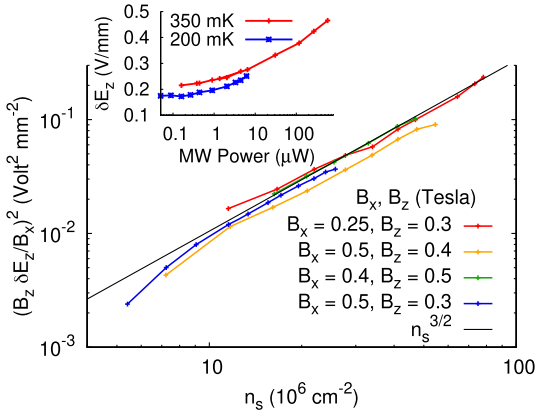

FIG. 4. The dependence of the squared linewidth scaled by the ratio of the magnetic fields $B_\parallel \equiv B_x$ and $B_\perp \equiv B_z$ on the electron density n_s. The excitation frequency is 174 GHz except for the data at $B_\perp \equiv B_z = 0.3$ T, which refers to $f = 144$ GHz. The black line shows the prediction of Eq. (4) for the effective electron temperature $T_e = 0.6$ K. Inset: the linewidth as a function of the microwave power for $B_z = 0.5$ T, $B_x = 0.75$ T, $f = 150$ GHz, and $n_s = 21.5 \times 10^6$ cm^{-2}.

By rescaling the linewidth, we see that the results for different $B_\parallel$ and $B_\perp$ collapse onto the same curve.

The many-electron theory of the interband absorption spectra developed in this Letter and the experimental observations are in full quantitative agreement, with no adjustable parameters. In contrast to the previous work on the electron absorption spectra, the theory explicitly takes into account strong electron correlations. The experimental data were obtained by extending the measurements to low microwave power, which made it possible to investigate the spectra in the linear-response regime.

The experimental data provide the first direct measurement of the fluctuational electric field which an electron is experiencing in a nondegenerate electron liquid and which, as we show, determines the shape of the spectrum. The results refer to a broad range of the electron densities, temperature, and the coupling strength of the in-plane and out-of-plane motions, where the in-plane motion is quantized by the magnetic field. Such quantization is advantageous for revealing nontrivial aspects of the many-electron dynamics in a strongly correlated two-dimensional system.

Our results demonstrate that, by applying an in-plane magnetic field, one can directly study intimate features of the quantum physics of an electron liquid and a Wigner crystal. The regimes other than the one explored here experimentally can be also investigated with the developed technique. Those include the regime of Wigner crystallization, in which case the closed-form expression for the spectrum is obtained. Self-diffusion in the electron liquid, which is hard to characterize otherwise, can be also explored. Importantly, the results demonstrate that electrons on helium can be used as a test bed for the quantum theory of the effect of the electron-phonon coupling on the optical spectra of color centers. The system provides a unique setting where both the effective coupling strength and the spectrum of elementary excitations coupled to the electron transition can be varied *in situ* by varying the in-plane and out-of-plane magnetic fields.

A. D. C. acknowledges support from ANR JCJC SPINEX. D. K. is supported by the internal grant from the Okinawa Institute of Science and Technology (OIST) Graduate University. M. I. D. was supported in part by the Grant No. DE-SC0020136 funded by the U.S. Department of Energy, Office of Science.

[1] *Two-Dimensional Electron Systems on Helium and Other Cryogenic Surfaces*, edited by E. Andrei (Kluwer Academic, Dordrecht, 1997).

[2] Y. Monarkha and K. Kono, *Two-Dimensional Coulomb Liquids and Solids* (Springer, Berlin, 2004).

[3] C. C. Grimes, T. R. Brown, M. L. Burns, and C. L. Zipfel, Spectroscopy of electrons in image-potential-induced surface states outside liquid helium, Phys. Rev. B **13**, 140 (1976).

[4] F. Stern, Image potential near a gradual interface between two dielectrics, Phys. Rev. B **17**, 5009 (1978).
[5] D. K. Lambert and P. L. Richards, Measurement of Local Disorder in a Two-Dimensional Electron Fluid, Phys. Rev. Lett. **44**, 1427 (1980).
[6] M. V. Rama Krishna and K. B. Whaley, Excess-electron surface states of helium clusters, Phys. Rev. B **38**, 11839 (1988).
[7] E. Cheng, M. W. Cole, and M. H. Cohen, Binding of electrons to the surface of liquid helium, Phys. Rev. B **50**, 1136 (1994).
[8] E. Collin, W. Bailey, P. Fozooni, P. G. Frayne, P. Glasson, K. Harrabi, M. J. Lea, and G. Papageorgiou, Microwave Saturation of the Rydberg States of Electrons on Helium, Phys. Rev. Lett. **89**, 245301 (2002).
[9] M. H. Degani, G. A. Farias, and F. M. Peeters, Bound states and lifetime of an electron on a bulk helium surface, Phys. Rev. B **72**, 125408 (2005).
[10] D. Konstantinov, M. I. Dykman, M. J. Lea, Y. Monarkha, and K. Kono, Resonant Correlation-Induced Optical Bistability in an Electron System on Liquid Helium, Phys. Rev. Lett. **103**, 096801 (2009).
[11] M. I. Dykman, K. Kono, D. Konstantinov, and M. J. Lea, Ripplonic Lamb Shift for Electrons on Liquid Helium, Phys. Rev. Lett. **119**, 256802 (2017).
[12] K. M. Yunusova, D. Konstantinov, H. Bouchiat, and A. D. Chepelianskii, Coupling between Rydberg States and Landau Levels of Electrons Trapped on Liquid Helium, Phys. Rev. Lett. **122**, 176802 (2019).
[13] A. M. Stoneham, *Theory of Defects in Solids* (Oxford University Press, Oxford, 2001).
[14] D. D. Awschalom, R. Hanson, J. Wrachtrup, and B. B. Zhou, Quantum technologies with optically interfaced solid-state spins, Nat. Photonics **12**, 516 (2018).
[15] P. M. Platzman and M. I. Dykman, Quantum computing with electrons floating on liquid helium, Science **284**, 1967 (1999).
[16] S. A. Lyon, Spin-based quantum computing using electrons on liquid helium, Phys. Rev. A **74**, 052338 (2006).
[17] D. I. Schuster, A. Fragner, M. I. Dykman, S. A. Lyon, and R. J. Schoelkopf, Proposal for Manipulating and Detecting Spin and Orbital States of Trapped Electrons on Helium Using Cavity Quantum Electrodynamics, Phys. Rev. Lett. **105**, 040503 (2010).
[18] G. Yang, A. Fragner, G. Koolstra, L. Ocola, D. A. Czaplewski, R. J. Schoelkopf, and D. I. Schuster, Coupling an Ensemble of Electrons on Superfluid Helium to a Superconducting Circuit, Phys. Rev. X **6**, 011031 (2016).
[19] H. Byeon, K. Nasyedkin, J. R. Lane, N. R. Beysengulov, L. Zhang, R. Loloee, and J. Pollanen, Piezoacoustics for flying electron qubits on helium, arXiv:2008.02330.
[20] C. C. Grimes and G. Adams, Evidence For A Liquid-to-Crystal Phase-Transition In A Classical, 2-Dimensional Sheet of Electrons, Phys. Rev. Lett. **42**, 795 (1979).
[21] D. S. Fisher, B. I. Halperin, and P. M. Platzman, Phonon-Ripplon Coupling and the 2-Dimensional Electron Solid On A Liquid-Helium Surface, Phys. Rev. Lett. **42**, 798 (1979).
[22] M. I. Dykman and L. S. Khazan, Effect of the Interaction between Nondegenerate Electrons Localized in a Thin Surface Layer on the Cyclotron Resonance and on the Magnetoconductance, Sov. Phys. JETP **50**, 747 (1979).
[23] V. S. Edelman, Levitating electrons, Sov. Phys. Usp. **23**, 227 (1980).
[24] L. Wilen and R. Giannetta, Cyclotron-resonance of the 2d electron crystal, Surf. Sci. **196**, 24 (1988).
[25] M. I. Dykman, M. J. Lea, P. Fozooni, and J. Frost, Magnetoresistance In 2D Electrons On Liquid-Helium—Many-Electron Versus Single-Electron Kinetics, Phys. Rev. Lett. **70**, 3975 (1993).
[26] A. Kristensen, K. Djerfi, P. Fozooni, M. J. Lea, P. J. Richardson, A. Santrich-Badal, A. Blackburn, and R. W. van der Heijden, Hall-Velocity Limited Magnetoconductivity in a Classical Two-Dimensional Wigner Crystal, Phys. Rev. Lett. **77**, 1350 (1996).
[27] D. Konstantinov, Y. Monarkha, and K. Kono, Effect of Coulomb Interaction on Microwave-Induced Magnetoconductivity Oscillations of Surface Electrons on Liquid Helium, Phys. Rev. Lett. **111**, 266802 (2013).
[28] A. D. Chepelianskii, M. Watanabe, K. Nasyedkin, K. Kono, and D. Konstantinov, An incompressible state of a photo-excited electron gas, Nat. Commun. **6**, 7210 (2015).
[29] D. G. Rees, N. R. Beysengulov, J.-J. Lin, and K. Kono, Stick-Slip Motion of the Wigner Solid on Liquid Helium, Phys. Rev. Lett. **116**, 206801 (2016).
[30] J. F. Barry, J. M. Schloss, E. Bauch, M. J. Turner, C. A. Hart, L. M. Pham, and R. L. Walsworth, Sensitivity optimization for NV-diamond magnetometry, Rev. Mod. Phys. **92**, 015004 (2020).
[31] M. K. Bhaskar, R. Riedinger, B. Machielse, D. S. Levonian, C. T. Nguyen, E. N. Knall, H. Park, D. Englund, M. Lončar, D. D. Sukachev, and M. D. Lukin, Experimental demonstration of memory-enhanced quantum communication, Nature (London) **580**, 60 (2020).
[32] T. Ando, A. B. Fowler, and F. Stern, Electronic-Properties of two-dimensional systems, Rev. Mod. Phys. **54**, 437 (1982).
[33] C. L. Zipfel, T. R. Brown, and C. C. Grimes, Spectroscopic studies of electron surface states on liquid helium, Surf. Sci. **58**, 283 (1976).
[34] C. L. Zipfel, T. R. Brown, and C. C. Grimes, Measurement of the Velocity Autocorrelation Time in a Two-Dimensional Electron Liquid, Phys. Rev. Lett. **37**, 1760 (1976).
[35] S. I. Pekar, Theory of color centers, Zh. Eksp. Teor. Fiz. **20**, 510 (1950).
[36] K. Huang and A. Rhys, Theory of light absorption and non-radiative transitions in F-centres, Proc. R. Soc. A **204**, 406 (1950).
[37] See Supplemental Material at http://link.aps.org/supplemental/10.1103/PhysRevLett.127.016801 for details of the calculation and the measurements, which includes Refs. [38–43].
[38] D. K. Lambert and P. L. Richards, Far-infrared and capacitance measurements of electrons on liquid helium, Phys. Rev. B **23**, 3282 (1981).
[39] F. Ulinich and N. Usov, Phase diagram of a two-dimensional Wigner crystal in a magnetic field, Sov. Phys. JETP **49**, 147 (1979).
[40] C. Fang Yen, M. I. Dykman, and M. J. Lea, Internal forces in nondegenerate two-dimensional electron systems, Phys. Rev. B **55**, 16272 (1997).

[41] K. Moskovtsev and M. I. Dykman, Self-diffusion in a spatially modulated system of electrons on helium, J. Low Temp. Phys. **195**, 266 (2019).

[42] W. T. Sommer and D. J. Tanner, Mobility of electrons on the surface of liquid He4, Phys. Rev. Lett. **27**, 1345 (1971).

[43] M. J. Lea, P. Fozooni, A. Kristensen, P. J. Richardson, K. Djerfi, M. I. Dykman, C. Fang-Yen, and A. Blackburn, Magnetoconductivity of two-dimensional electrons on liquid helium:Experiments in the fluid phase, Phys. Rev. B **55**, 16280 (1997).